Proc. Natl. Acad. Sci. USA
Vol. 84, pp. 7957–7961, November 1987
Cell Biology

Ligands internalized through coated or noncoated invaginations follow a common intracellular pathway

(endocytosis/endosomes)

DIEN TRAN*†, JEAN-LOUIS CARPENTIER*, FUMIO SAWANO*, PHILLIP GORDEN‡, AND LELIO ORCI*

*Institute of Histology and Embryology, University Medical Center, 1211 Geneva 4, Switzerland; and ‡Diabetes Branch, National Institute of Diabetes and Digestive and Kidney Diseases, National Institutes of Health, Bethesda, MD 20892

Communicated by J. E. Rall, June 22, 1987 (received for review April 9, 1987)

ABSTRACT **Cholera toxin (CT) represents a class of ligands that binds preferentially to noncoated pits on the cell surface. In the present study, we have investigated the mechanism of endocytosis of this class of ligand and compared it to the classic coated pit mechanism. When either CT coupled to colloidal gold particles (CT–gold) or ^{125}I-labeled CT were incubated with 3T3 L1 fibroblasts at 4°C, both ligands bound in a preferential fashion to small noncoated pits on the cell surface. CT–gold surface-labeled cells were then incubated at 22°C. The labeled ligand progressively moved into noncoated vesicles and a tubulovesicular compartment composed of a network of tubules and vesicles closely associated with multivesicular bodies but distinct from the Golgi complexes. The ligand next passed into multivesicular bodies. By contrast, α_2-macroglobulin (α_2m)–gold initially localized preferentially to coated pits and subsequently to coated vesicles and tubulovesicular structures before associating with multivesicular bodies. To directly compare the intracellular pathway followed by CT–gold to that followed by α_2m–gold, CT–gold (7 nm) was coincubated with α_2m–gold (15 nm). By 10 min of incubation at 22°C, up to 66% of tubulovesicular units contained both ligands when analyzed in serial sections. Subsequently, both ligands were colocalized in multivesicular bodies. We conclude that CT–gold endocytosed via noncoated vesicles and α_2m–gold endocytosed through coated vesicles subsequently associate with the same tubulovesicular units, multivesicular bodies, and lysosomes.**

Adsorptive endocytosis is a process by which cells selectively concentrate and internalize ligands that bind to plasma membrane receptors. In most instances, this process is accomplished through the clustering of receptor-bound ligands in clathrin-coated indentations of the cell surface known as coated pits and through the subsequent formation of coated vesicles (1, 2). Recently, however, it has been proposed that some ligands do not bind or cluster in coated pits and are internalized through noncoated invaginations of the plasma membrane. This suggestion was based on the observation that the preferential association of cholera toxin (CT)–gold, tetanus toxin-gold, and anti-HLA antibody with noncoated invaginations of the cell surface is followed by the internalization of these ligands (3, 4).

The intracellular pathway followed by ligands internalized through coated pits has been extensively studied; it is now generally accepted that within seconds to minutes coated vesicles are formed, the coat is lost, and larger smooth-surfaced vacuoles with ligand (endosomes) are found. Later, the ligand associates with multivesicular bodies and eventually with more typical lysosomes (1, 2, 5). By contrast, the pathway followed by ligands thought to be internalized through noncoated pits remains obscure.

The publication costs of this article were defrayed in part by page charge payment. This article must therefore be hereby marked "*advertisement*" in accordance with 18 U.S.C. §1734 solely to indicate this fact.

In the present study, we have addressed three questions. (*i*) Does a quantitative analysis involving the use of the same ligand tagged with a different morphological probe confirm that noncoated invaginations are involved in receptor-mediated endocytosis of specific ligands? (*ii*) If so, what is the intracellular pathway followed by these ligands? (*iii*) Does this pathway differ from the pathway followed by ligands internalized through coated pits?

MATERIAL AND METHODS

Cell Culture and Reagents. 3T3 L1 fibroblasts were generously provided by Ora M. Rosen (Albert Einstein College of Medicine, New York, NY). The cells were grown to confluence in 35-mm Petri dishes as described (6).

CT (Calbiochem) was iodinated by the chloramine-T method according to Bennett and Cuatrecasas (7). α_2-Macroglobulin (α_2m) was from Boehringer Mannheim.

Colloidal gold particles (15 nm) were prepared according to Frens (8) while smaller particles (≈7 nm) were prepared according to Mühlpfordt (9). The method used for coupling colloidal gold to proteins has been described (10).

Incubation Conditions and Processing for Electron Microscopy. Cells were first incubated for 1 hr at 37°C in serum-free medium to remove most of the cellular bound α_2m derived from fetal calf serum, and then washed extensively at 4°C with Krebs–Ringer bicarbonate (KRB) buffer containing 3% bovine serum albumin (fraction V) (pH 7.4). The cell temperature was equilibrated at 4°C for 15 min.

Cells were further incubated in 1 ml of KRB (pH 7.4) containing the labeled ligand [≈100 μg of α_2m–gold per ml or ≈1.30 μg of CT–gold per ml, or ≈10 ng of ^{125}I-labeled CT (^{125}I-CT) per ml] for 2 hr at 4°C. Cells were then washed three times with KRB buffer (pH 7.4) at 4°C and further incubated for various periods of time at 22°C in the absence of labeled ligand. To determine nonspecific binding (cell-associated labeled ligand in the presence of excess unlabeled ligand), 100 μg of CT per ml or 5 mg of α_2m per ml was used. Nonspecific binding was ≈2% for α_2m–gold and ≈10% for ^{125}I-CT or CT–gold (11).

At each incubation time studied, cells were washed three times in KRB buffer (pH 7.4), before being fixed for 30 min at room temperature in 2.5% glutaraldehyde/0.1 M cacodylate buffer, pH 7.4. The preparations were then washed three times in 0.1 M cacodylate buffer (pH 7.4), postfixed in 1% osmium tetroxide in Veronal acetate buffer (pH 7.4) for 20 min at room temperature, and treated with 0.5% tannic acid (tannic acid AR, code no. 1764; Mallinckrodt) in 50 mM cacodylate buffer (pH 7.0) for <1 min. Thus, when cell

Abbreviations: CT, cholera toxin; α_2m, α_2-macroglobulin; ^{125}I-CT, ^{125}I-labeled CT.

†On leave from Institut National de la Santé et de la Recherche Medicale U12, Scholarship of the "Fondation pour la Recherche Médicale," France.

membranes were accessible to tannic acid, those membranes were highlighted. They were then stained en bloc with 0.5% uranyl acetate in Veronal acetate buffer for 20 min, dehydrated in graded ethanols, and embedded in Epon. Thin sections were cut either parallel or perpendicular to the plane of the culture.

Quantitative Analysis. The determination of the percentage of gold particles associated with the various surface and intracellular structures considered was carried out on a total of 100 pictures per time point in each experiment. These pictures, printed so as to reach a final magnification of ×60,000, were taken on the basis of the first 100 labeled structures encountered in a minimum of three different Epon blocks for each condition. Thus, a minimum of 50 different cells per time point in each experimental condition was studied. For each gold ligand analyzed, three different experiments were carried out.

When double-labeling experiments were performed, an additional analysis evaluated the percentage of structures labeled with both ligands in terms of the total number of structures labeled.

All determinations for quantitative electron microscope autoradiography were carried out as described (12).

RESULTS

Surface Distribution and Intracellular Pathway Followed by CT–Gold. Following a 2-hr incubation at 4°C in the presence of CT–gold (7 or 15 nm), a large percentage of the surface-bound colloidal gold particles were associated with apparently undifferentiated segments of the surface of 3T3 L1 fibroblasts, while 15–20% of the CT–gold complexes were found in small noncoated invaginations (Fig. 1). This observation was repeated by quantitative electron microscope autoradiography using ^{125}I-CT (data not shown), and for both labeled ligands (CT–gold or ^{125}I-CT) we found a preferential association with these noncoated pits (Fig. 2) (ratio of percent labeled ligand associated with noncoated pits over percent cell surface occupied by noncoated pits: 3.4 and 4.2, respectively) but not with coated pits (ratios: 0.4 and 0.6, respectively).

Further incubation of the surface-labeled cells at 22°C resulted in a progressive increase in the percentage of colloidal gold particles associated with noncoated invaginations, which paralleled the decreased association of the ligand with undifferentiated regions of the plasma membrane (Fig. 1). The association with noncoated invaginations peaked by 10–20 min and then plateaued or slightly decreased (Fig. 1). This surface redistribution of CT–gold was accompanied by a progressive internalization of the labeled ligand, which first associated with vesicles of a similar diameter as noncoated invaginations (Fig. 2). At later incubation times, the CT–gold progressively accumulated in noncoated vesicles (which can be distinguished from noncoated pits by the absence of tannic acid labeling) and the tubulovesicular network (Figs. 1 and 2). Since noncoated vesicles could hardly be distinguished from transverse sections of tubules, these two compartments were pooled for the quantitative analysis. The association of CT–gold with this tubulovesicular network reached a maximum by 20 min of incubation at 22°C and then decreased while the ligand gold complexes progressively accumulate within multivesicular bodies (Figs. 1 and 2).

A similar sequence of events occurred over an identical time frame when 3T3 L1 fibroblasts were incubated with CT coupled to 7-nm colloidal gold particles or with ^{125}I-CT (data not shown). These observations validate the use of CT–gold conjugates. When the incubation was carried out at 37°C, a larger percentage of the CT–gold was internalized than at 22°C. Under these conditions, the same structures as the one previously described were involved in the internalization

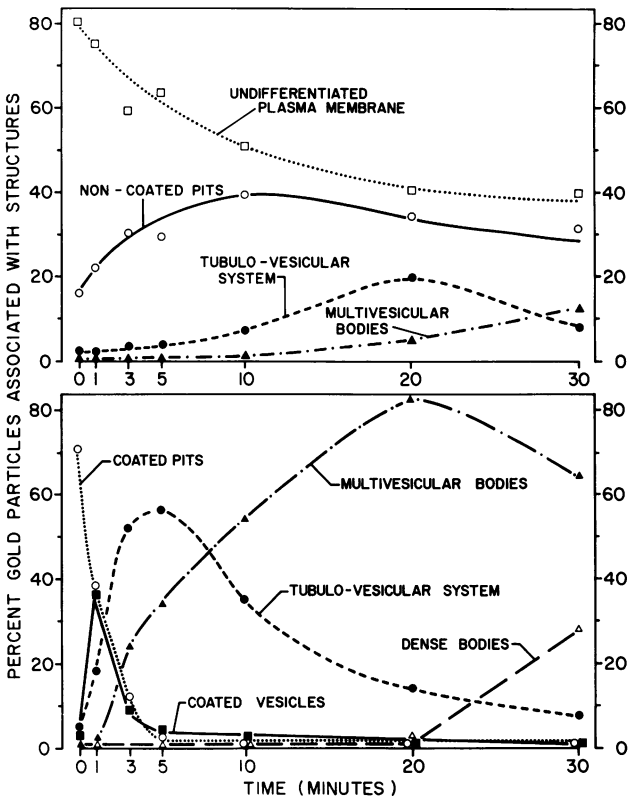

FIG. 1. Relationship of CT–gold (*Upper*) and α_2m–gold (*Lower*) with the various surface and intracellular compartments of 3T3 L1 fibroblasts surface-labeled for 2 hr at 4°C and further incubated in the absence of labeled ligand at 22°C. At each time point, the first 100 labeled structures were photographed and the percentage of the total number of gold particles associated with each compartment was calculated.

process and the association with the tubulovesicular system peaked by 10 min of incubation (data not shown).

Surface Binding and Intracellular Pathway Followed by α_2m–Gold. The sequence of events followed by CT–gold after its binding to 3T3 L1 fibroblasts was compared to that followed by a ligand known to preferentially associate with and to be internalized through coated pits, α_2m. This ligand was coupled to 15-nm colloidal gold particles and incubated with 3T3 L1 fibroblasts following the same experimental protocol as that described for CT–gold. By 2 hr of incubation at 4°C, the labeled ligand was associated with the plasma membrane where >70% of gold particles were found in coated segments (Figs. 1 and 3). Coated pits were distinguished from coated vesicles by the presence or absence of tannic acid (Figs. 3 and 4). When surface-labeled fibroblasts were incubated at 22°C in the absence of ligand, by 1 min of incubation half of the α_2m–gold was internalized and recovered in coated vesicles (Figs. 1 and 3). As a function of incubation time, α_2m–gold progressively accumulated in a tubulovesicular network similar to that observed in the course of CT–gold internalization. The next intracellular compartment to be labeled included multivesicular bodies (Figs. 1 and 3).

Double-Labeling Experiments. We wished next to determine whether both CT–gold and α_2m–gold were conveyed through the same or distinct tubulovesicular unit(s). To answer this question, CT–gold (7 nm) and α_2m–gold (15 nm) were concomitantly added to the incubation medium of 3T3 L1 fibroblasts. The percentage of labeled structures containing both CT–gold (7 nm) and α_2m–gold (15 nm) increased with incubation time at 22°C so that by 10 min when most CT–gold is associated with the tubulovesicular units and when α_2m–

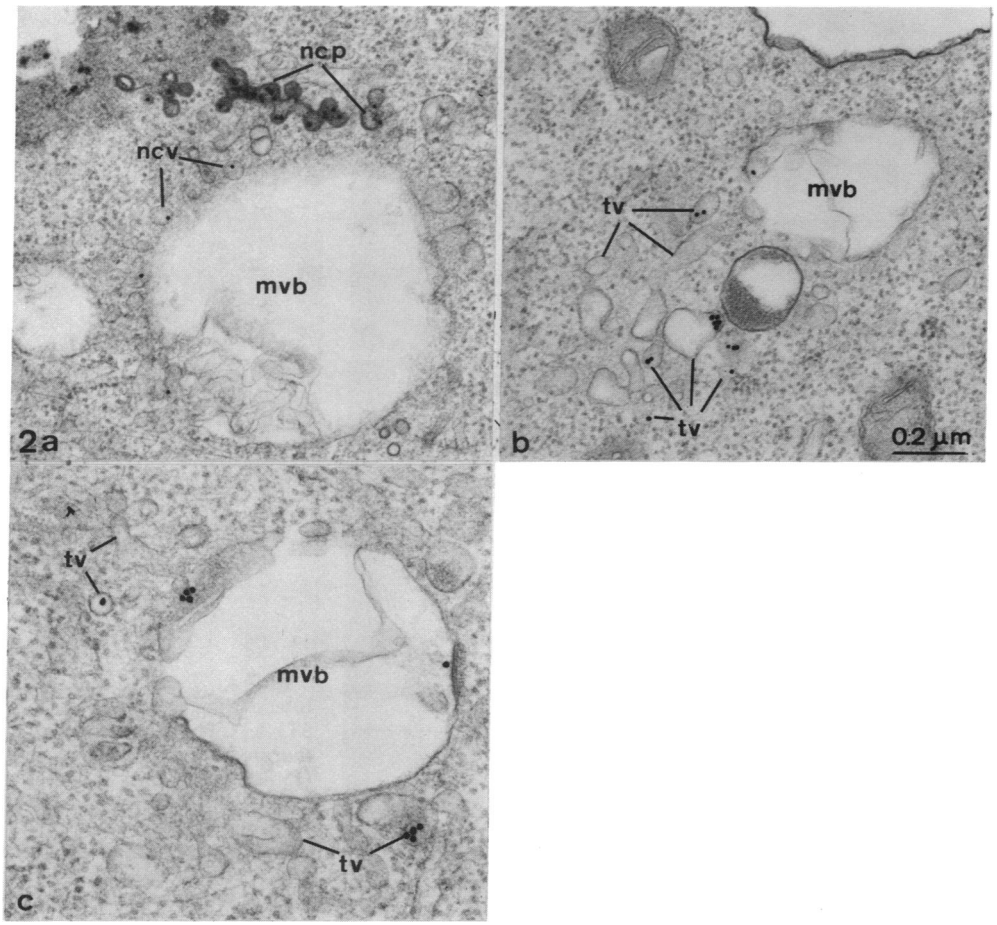

FIG. 2. Representative examples of surface and intracellular structures with which CT–gold (15 nm) associates in 3T3 L1 fibroblasts. In 5 min at 22°C, CT–gold complexes are associated with noncoated pits (ncp) (stained with tannic acid) and with noncoated vesicles (ncv) (negative for tannic acid), which are near tubulovesicular structures. In *b* and *c* (10 and 20 min, 22°C), CT–gold complexes are associated with a network of tubulovesicular structures (tv), which are in close relationship with multivesicular bodies (mvb). These tubules and vesicles are grouped in a limited region of the cell periphery so as to form a tubulovesicular unit. (*a*, ×40,000; *b*, ×27,000; *c*, ×46,000.)

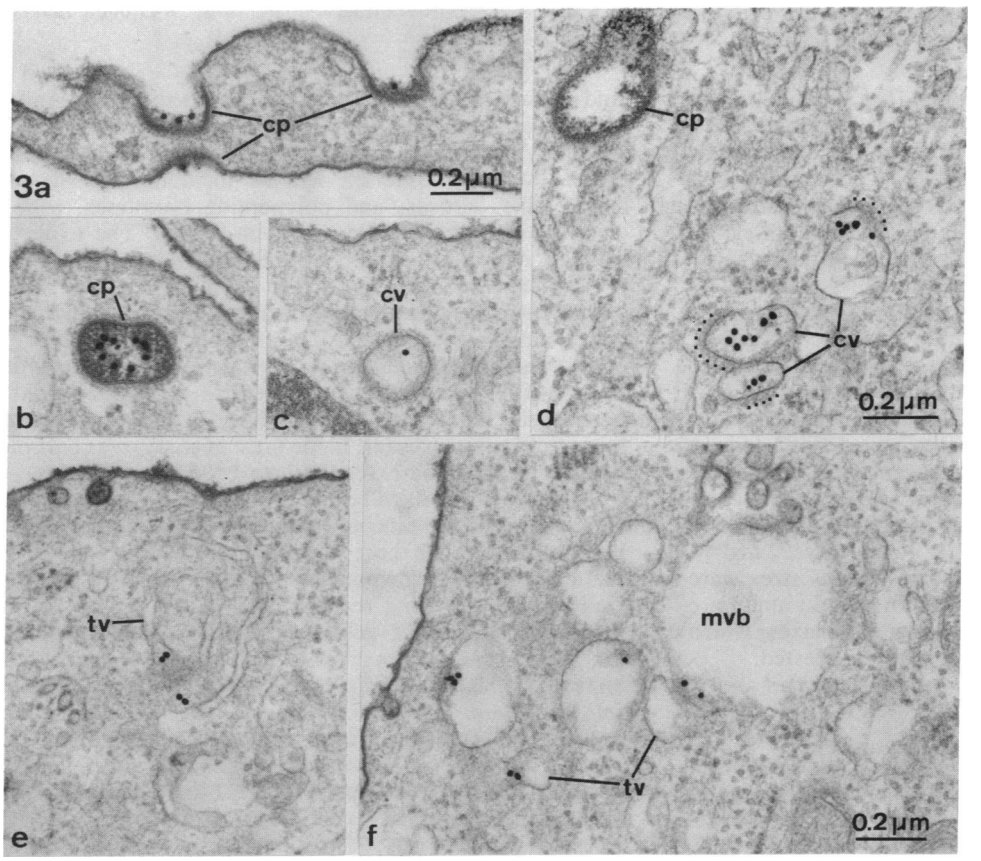

FIG. 3. Representative examples of surface and intracellular compartments with which α_2m–gold (15 nm) associates in 3T3 L1 fibroblasts. In *a* and *b* (2 hr at 4°C), α_2m–gold complexes preferentially associate with coated pits (cp) on the cell surface. The surface connections of these structures are verified by their tannic acid labeling (*b*). In *c* (1 min at 22°C), α_2m–gold complexes are recovered in coated vesicles (cv) lacking any staining with tannic acid. In *d* (3 min at 22°C), α_2m–gold associates with partially coated structures (underlined with black dots) and later (*e*), it is progressively localized in tubulovesicular structures (tv) frequently neighbored by multivesicular bodies (mvb) (*f*). (*a*, ×41,000; *b*, ×49,000; *c*, ×49,000; *d*, ×49,000; *e*, ×43,000; *f*, ×46,000.)

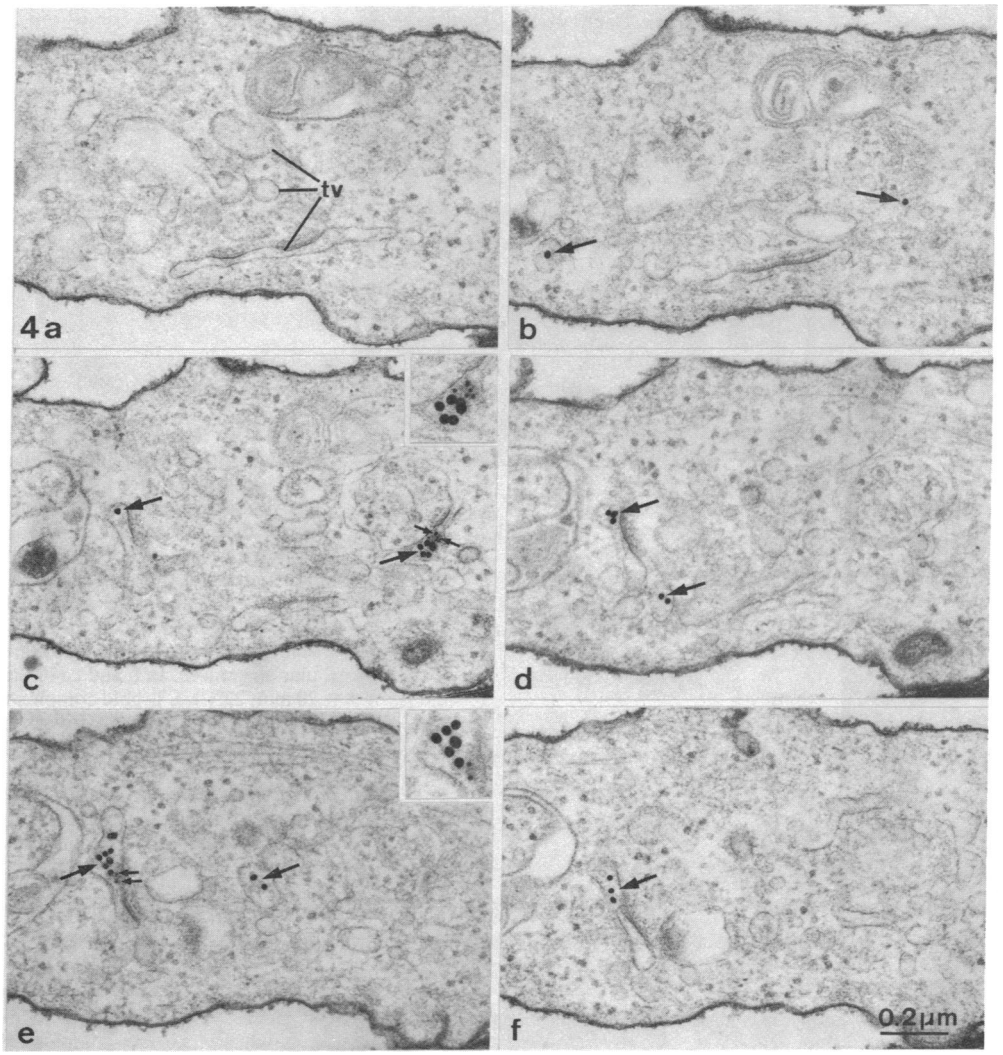

FIG. 4. Serial sections of a tubulovesicular unit (tv) from a 3T3 L1 fibroblast incubated in the presence of both α_2m–gold (15 nm) (large arrows) and CT–gold (7 nm) (small arrows). Tubules and vesicles, which appear labeled with a single ligand in a plane of section, can contain both ligands as demonstrated by serial sections. Note that the cytoplasmic leaflet of the tubulovesicular structures is frequently underlined by a fuzzy coat. (*a–f*, ×43,000; *Insets*, ×79,000.)

gold is still present in this compartment (see above), 15% of the labeled structures contained both ligands in a single plane of section. This is a minimal estimate since quantitative analysis carried out on serial sections of 75 different tubulovesicular units labeled with either CT–gold (7 nm) or α_2m–gold (15 nm) demonstrates that by 10 min of incubation, 50 of these tubulovesicular units (66%) contain the other labeled ligand in a subsequent section of the same intracellular compartment (Fig. 4). These data support the notion that ligands internalized through coated or noncoated invaginations are channeled through the same tubulovesicular units.

Morphological Characteristics of the Tubulovesicular System. Within 3T3 L1 fibroblasts, the tubulovesicular system is composed of several units, each occupying a defined domain of the peripheral cytoplasm. In a single section, a mean of three tubulovesicular units is detected. Each unit is composed of an interconnected network of tubules and vesicles closely associated with multivesicular bodies (Figs. 2 and 4). Partially or totally coated structures of various sizes were frequently present (Fig. 4). The tubulovesicular units are moreover clearly distinct from the Golgi complexes, which remain unlabeled by both gold-labeled ligands tested.

DISCUSSION

Morphologically three distinct or partially overlapping types of endocytosis have been identified. These include (*i*) adsorptive endocytosis occurring through coated pits, (*ii*) adsorptive endocytosis occurring through noncoated pits, and (*iii*) fluid phase endocytosis. Since the classic studies of Anderson, Brown, and Goldstein, it has become clear that coated pits are a preferential pathway for receptor-mediated endocytosis of many different ligands including low density lipoproteins, viruses, and polypeptide hormones. α_2m is highly representative of this system (1, 13). The expected behavior of α_2m is further confirmed in 3T3 fibroblasts in the present experiments.

By contrast, noncoated surface invaginations have been considered as dynamic structures involved in fluid-phase endocytosis (2). Recently, it has been demonstrated that these surface invaginations preferentially bound CT–gold, a ligand that binds to GM1 gangliosides (14) and tetanus toxin–gold complexes (4). In the present study, we confirmed this observation and extended it to ^{125}I-CT.

Only 0.5% of surface bound CT–gold particles are associated with coated pits and this small fraction could be internalized through these structures. It is unlikely, however, that coated pits are responsible for most of the CT internalized for the following reasons: (*i*) By the end of the 4°C incubation 0.5% of CT–gold complexes associate with coated pits but this association drops to 0 within 1–3 min at 22°C. In spite of that, internalization of CT–gold complexes proceeds for 10–30 min. (*ii*) We were unable to detect a significant association of CT–gold with coated vesicles at any time studied in spite of the slow internalization of this ligand. By contrast, following internalization, CT–gold complexes rapidly associate with noncoated vesicles of a size identical to that of noncoated pits. These observations suggest that the

small noncoated invaginations to which CT preferentially binds are part of the endocytotic process that mediates the internalization of CT.

Endosomes comprise a heterogenous population of vesicles and tubules, which are important sorting centers from which materials may be directed to lysosomes, back to the cell surface, to the extracellular space, or to the cytosol (1, 2). Previous studies have clearly demonstrated that ligands utilizing different receptors enter the same coated pits and consequently the same endosome (13, 15). Assuming that the tubulovesicular units represent the endosomes, the present data extend this concept to ligands associated with noncoated pits, which reach the same endosomes as those through which ligands internalized via coated pits are channeled. Endosomes appear to be a meeting point for any material internalized by adsorptive endocytosis. This material is then by unknown mechanisms sorted and routed in the appropriate direction. It has recently been suggested that fluid phase markers transit within endosomes together with receptor-bound ligands (16, 17).

Subsequent to the endosomal step, both α_2m and CT accumulate in a time-dependent manner in the same multivesicular bodies. By contrast, no labeling was found in Golgi-associated vesicles or Golgi cisternae at any time interval (up to 30 min). These findings differ from those of Joseph *et al.* (18) and Hanover *et al.* (19) inasmuch as they reported that horseradish peroxidase-conjugated CT and α_2m associate with the Golgi compartment before being delivered to lysosomes. Although it has been suggested that the morphologic probe *per se* may alter the intracellular location of certain ligands (20, 21), it is unlikely to affect the results presented here: (*i*) because the movement of α_2m is similar to what has been seen with other ligands in most cell types (1, 2, 5) and (*ii*) the behavior of CT–gold is qualitatively similar to what was observed with ^{125}I-CT both at the cell surface and intracellularly.

The internalization of both CT–gold and α_2m–gold is time and temperature dependent with the rate of internalization of both ligands being greater at 37°C than at 22°C. The relative rates, however, are very different inasmuch as α_2m is internalized much more efficiently (i.e., $\approx$4 times as fast) than is CT–gold at both 22°C and 37°C.

The present study defines the endocytotic pathway of a ligand that preferentially binds to small noncoated invaginations on the cell surface. Furthermore, the data demonstrate the high degree of overlap at the earliest identifiable endocytotic step between this pathway and the coated pit pathway. These initial endosomal structures are situated in discrete units distinct from the Golgi complexes; they do not contain lysosomal enzymes (data not shown) but are intimately associated with multivesicular bodies. Thus, the endocytotic pathways for two different types of ligands are distinct at the cell surface but become more redundant as ligand is transferred intracellularly.

The authors are indebted to Ms. G. Berthet and N. Dupont for skilled technical and typographical assistance. This investigation was supported by Grant 3.404.86 from the Swiss National Science Foundation.

1. Goldstein, J. L., Brown, M. S., Anderson, R. G. W., Russel, D. N. & Schneider, W. J. (1985) *Annu. Rev. Cell Biol.* **1**, 1–39.
2. Steinman, R. M., Mellman, I. S., Muller, W. A. & Cohn, Z. A. (1983) *J. Cell Biol.* **96**, 1–27.
3. Huet, C., Ash, J. F. & Singer, S. J. (1980) *Cell* **21**, 429–436.
4. Montesano, R., Roth, J., Robert, A. & Orci, L. (1982) *Nature (London)* **296**, 651–653.
5. Gorden, P., Carpentier, J.-L. & Orci, L. (1985) in *Diabetes and Metabolism Reviews*, ed. De Fronzo, R. A. (Wiley, New York), Vol. 1, pp. 99–117.
6. Fan, J. Y., Carpentier, J.-L., Gorden, P., Van Obberghen, E., Blackett, N. M., Grunfeld, C. & Orci, L. (1982) *Proc. Natl. Acad. Sci. USA* **79**, 7788–7791.
7. Bennett, V. & Cuatrecasas, P. (1975) *J. Membr. Biol.* **22**, 29–52.
8. Frens, G. (1973) *Nature (London) Phys. Sci.* **241**, 20–22.
9. Mühlpfordt, M. (1982) *Experientia* **38**, 1127–1128.
10. Roth, J. (1982) in *Techniques in Immunocytochemistry*, eds. Bullock, G. & Petrusz, P. (Academic, New York), Vol. 1, pp. 107–133.
11. Carpentier, J.-L., Rees, A. R., Gregoriou, M., Kris, R., Schlessinger, J. & Orci, L. (1986) *Exp. Cell Res.* **166**, 311–326.
12. Carpentier, J.-L., Gorden, P., Amherdt, M., Van Obberghen, E., Kahn, C. R. & Orci, L. (1978) *J. Clin. Invest.* **61**, 1057–1070.
13. Dickson, R. B., Willingham, M. C. & Pastan, I. (1981) *J. Cell Biol.* **89**, 29–34.
14. Fishman, P. M. (1982) *J. Cell Biol.* **93**, 860–865.
15. Carpentier, J.-L., Gorden, P., Anderson, R. G. W., Goldstein, J. L., Brown, M. S., Cohen, S. & Orci, L. (1982) *J. Cell Biol.* **95**, 73–77.
16. Gonatas, N. K., Stieber, A., Hickey, W. F., Herbert, S. H. & Gonatas, J. O. (1984) *J. Cell Biol.* **99**, 1379–1390.
17. Neutra, M. R., Ciechanover, A., Owen, L. S. & Lodish, H. F. (1985) *J. Histochem. Cytochem.* **33**, 1134–1144.
18. Joseph, K. C., Stieber, A. & Gonatas, N. K. (1979) *J. Cell Biol.* **81**, 543–554.
19. Hanover, J. A., Willingham, M. C. & Pastan, I. (1984) *Cell* **39**, 283–293.
20. Gonatas, J., Stieber, A., Olsnes, S. & Gonatas, N. K. (1980) *J. Cell Biol.* **87**, 579–588.
21. Van Deurs, B., Tønnessen, T. I., Petersen, O. N., Sandvig, K. & Olsnes, S. (1986) *J. Cell Biol.* **102**, 37–47.